

Pseudoscalar mesons from a PNJL model at zero temperature

R. M. Aguirre¹ and O. Lourenço^{2,3}

¹*Departamento de Física, Facultad de Ciencias Exactas, Universidad Nacional de La Plata, and IFLP, UNLP-CONICET, C.C. 67 (1900) La Plata, Argentina*

²*Departamento de Física, Instituto Tecnológico de Aeronáutica, DCTA, 12228-900, São José dos Campos, SP, Brazil*

³*Université de Lyon, Université Claude Bernard Lyon 1, CNRS/IN2P3, IP2I Lyon, UMR 5822, F-69622, Villeurbanne, France*

(Dated: January 26, 2024)

We study pseudoscalar π , K and η meson properties, such as masses and couplings, in dense matter at zero temperature. We use a recently proposed phenomenological quark model, known as the PNJL0, which takes into account the confinement/deconfinement phase transition by means of the traced Polyakov loop (Φ) which serves as an order parameter at zero temperature. We consider two different scenarios, namely, symmetric quark matter with equal chemical potentials for all the flavors, and the beta equilibrated matter. In the latter case the hadron-quark phase transition is implemented by a two model approach. For the hadron side we use a relativistic mean-field model with density dependent couplings. We show that Φ induces abrupt changes in the mesons properties with gap sizes regulated by the phenomenological gluonic sector of the model.

I. INTRODUCTION

The study of meson properties under extreme conditions is expected to reveal significant features of the Quantum Chromodynamics (QCD) phase diagram [1]. For instance, the restoration of chiral symmetry at high temperatures would manifest by the degeneracy of the masses of the chiral partners $\sigma - \pi$ and a drastic drop of the effective coupling between pion and quarks [2, 3]. An interesting outcome is the prediction that mesonic excitations exist beyond the critical temperature for deconfinement and even for chiral symmetry restoration [2–8]. The enhanced fraction of bound states of strange quarks observed at high energies in heavy collisions at the Large Hadron Collider would give the experimental evidence. The situation may be consistently interpreted as a flavor staggered deconfinement [9]. This issue has been intensively studied for non-zero temperatures, leading to the conclusion that a coexistence of confined and deconfined phases [10, 11] is feasible. The simulations performed in [11] have shown that the collision of stable nuclei could produce a mixed phase at densities 3-4 times the normal nuclear density and temperatures around 50 MeV.

There are physical systems, as in the core of massive neutron stars, for which the coexistence of phases at nearly zero temperature is a plausible scenario [12]. The pure quark matter phase is also another possibility in this particular system [13, 14]. The relevance of the $T = 0$ and high density regime has been remarked by the finding of new phases in the QCD diagram, as for instance the kaon condensate for different flavor compositions [15], or in a superconducting quark matter state [16, 17].

The usual way to deal with a mixed phase is to use a dual scheme, taking hadrons as effective degrees of freedom below the threshold transition and a model of deconfined quarks above it. These different descriptions are combined in a continuous manner or not, depending on the nature of the transition. Furthermore, some hybrid models has been proposed that combine in the same

framework bound states and deconfined quarks, as for instance [18, 19]. In [18] the Polyakov loop is explicitly used, whereas [19] modifies the Fermi statistical distribution functions by restricting the momentum regime accessible for quarks or hadrons. By its very construction, the Polyakov loop has been used only for finite temperature situations. It has been recently proposed in Refs. [20–22] an extension of the Nambu-Jona Lasinio model (NJL) at zero temperature, with interacting quarks coupled to a scalar background field Φ that effectively mimics the quark-gluon dynamics, namely, the transition from strong to weak regimes of the quark-quark interaction. In such a model, called as PNJL0 model, it is possible to clearly determine different thermodynamical phases in which quarks are treated as confined or deconfined particles. Furthermore, the particular phase in which the system presents restored chiral symmetry, but with confined quarks, can also be identified. The back reaction between quark and gluon sectors is also a feature of the PNJL0 model. In Ref. [22] the thermodynamics of the 2-flavor version of the model was studied, and in Ref. [20] the extension to the SU(3) system was implemented with some applications to the stellar matter. More specifically, the construction of hybrid stars was analyzed in which the PNJL0 model was coupled to a hadronic relativistic mean-field (RMF) model.

Different studies have shown that the modification of the meson properties in a dense medium has significant consequences for a wide range of phenomena. In the astronomical scale, the condensation of pions and kaons in stars [23, 24] is a longstanding issue due to its influence on the cooling process [25] or the pulsar glitches. While in the microscopic scale, the phenomenology of mesic nuclei [26–32] has revealed some supporting evidence, as for instance the systematics of pionic nuclei which suggests a decrease of the pion decay constant [26]. Furthermore, calculations of a density dependent polarization insertion within a chiral inspired parametrization of hadronic masses or vertices predict stable configurations of nuclear

bound states of η [28, 30] as well as of η' mesons [31].

The combination of first principles and such phenomenological issues has given different theoretical pictures of the interaction between nucleons and the pseudoscalar mesons. Besides the well constrained nucleon-pion interaction, there is a variety of kaon models [33], as for instance effective kaon-meson [34] and chiral symmetry inspired kaon-nucleon [35, 36] vertices. The dynamics of the $\eta - \eta'$ system in a dense environment is less known, and its theoretical description has been mainly based on chiral constructions [37, 38], or relies on covariant hadronic field models [29, 32]. In this paper, we calculate the meson properties by using the PNJL0 model and a particular RMF hadronic one, both described in Sec. II. In Sec. III we present the theoretical framework for the evaluation of the meson polarization for both quark and hadronic models. The results for the masses and effective couplings of π , K , η mesons are shown and discussed in Sec. IV with special attention to the confinement/deconfinement phase transition. Finally, the summary and concluding remarks are presented in Sec. V.

II. PNJL0 MODEL: SYMMETRIC AND STELLAR MATTER CASES

The Lagrangian density that describes the three-flavor version of the PNJL model with scalar, vector, and 't Hooft channels is given by [20]

$$\begin{aligned} \mathcal{L}_{\text{PNJL}} = & \bar{q}(i\gamma_\mu D^\mu - \hat{m})q - \mathcal{U}(\Phi, \Phi^*, T) \\ & + \frac{G_s}{2} \sum_{a=0}^8 [(\bar{q}\lambda_a q)^2 - (\bar{q}\gamma_5 \lambda_a q)^2] \\ & - \frac{G_V}{2} \sum_{a=0}^8 [(\bar{q}\gamma_\mu \lambda_a q)^2 + (\bar{q}\gamma_\mu \gamma_5 \lambda_a q)^2] \\ & + K[\det_f(\bar{q}(1 - \gamma_5)q) + \det_f(\bar{q}(1 + \gamma_5)q)], \quad (1) \end{aligned}$$

where q is a vector of three spinors q_f for $f = u, d, s$, $D^\mu \equiv \partial^\mu + iA^\mu$ with $A^\mu = \delta_0^\mu A_0$ and $A_0 = gA_a^0 \lambda_a/2$ (g is the gauge coupling), $\hat{m} = \text{diag}(m_u, m_d, m_s)$ is a matrix of current quark masses in flavor space, and λ_a are the SU(3) Gell-Mann matrices. The strength of scalar, vector, and 't Hooft interactions is determined by the constants G_s , G_V , and K , respectively. The use of the mean-field approximation leads this quantity to

$$\begin{aligned} \mathcal{L}_{\text{PNJL}} = & \sum_f \bar{q}_f(i\gamma_\mu D^\mu - M_f)q_f - G_s \sum_f \rho_{sf}^2 \\ & + G_V \sum_f \rho_f^2 - 4K \prod_f \rho_{sf} - \mathcal{U}(\Phi, \Phi^*, T). \quad (2) \end{aligned}$$

Notice the inclusion of the Polyakov potential $\mathcal{U}(\Phi, \Phi^*, T)$ that depends on the traced Polyakov

loop, defined as

$$\begin{aligned} \Phi = & \frac{1}{3} \text{Tr} \left[\exp \left(i \int_0^{1/T} d\tau A_4 \right) \right] \\ = & \frac{1}{3} \left[e^{i(\phi_3 + \phi_s/\sqrt{3})} + e^{i(-\phi_3 + \phi_s/\sqrt{3})} + e^{-2i\phi_s/\sqrt{3}} \right], \quad (3) \end{aligned}$$

written in the Polyakov gauge where $\phi = \phi_3 \lambda_3 + \phi_8 \lambda_8$, and $A_4 = iA_0 \equiv T\phi$. Φ^* is the conjugate of Φ .

In general, the Polyakov potential is zero at $T = 0$, as one can see for instance in Refs. [39–42]. Therefore, all thermodynamical quantities related to the PNJL model reduces to the NJL model ones at this regime, and it is not possible to investigate deconfinement effects at this level. In order to make feasible such analysis, it was proposed in Refs. [20–22] the modification in the coupling constants of the model by making them functions of Φ as

$$G_s \rightarrow \mathcal{G}_s(G_s, \Phi) = G_s(1 - \Phi^2), \quad (4)$$

$$G_V \rightarrow \mathcal{G}_V(G_V, \Phi) = G_V(1 - \Phi^2), \quad (5)$$

$$K \rightarrow \mathcal{K}(K, \Phi) = K(1 - \Phi^2), \quad (6)$$

where we have used the approximation $\Phi = \Phi^*$ [20–22]. The motivation for these functions is to make vanishing all couplings at the limit of the deconfined phase, attained at $\Phi \rightarrow 1$. By taking into account these assumptions we generate the called PNJL0 model, for which pressure and energy density are respectively given, at $T = 0$, by

$$\begin{aligned} P_{\text{PNJL0}} = & -G_s \sum_f \rho_{sf}^2 + G_V \sum_f \rho_f^2 - 4K \prod_f \rho_{sf} \\ & + \frac{\gamma}{2\pi^2} \sum_f \int_0^\Lambda dk k^2 (k^2 + M_f^2)^{1/2} - \mathcal{U}(\rho_f, \rho_{sf}, \Phi) + \Omega_{\text{vac}} \\ & + \frac{\gamma}{6\pi^2} \sum_f \int_0^{k_{Ff}} \frac{dk k^4}{(k^2 + M_f^2)^{1/2}} \quad (7) \end{aligned}$$

and

$$\begin{aligned} \mathcal{E}_{\text{PNJL0}} = & G_s \sum_f \rho_{sf}^2 + G_V \sum_f \rho_f^2 + 4K \prod_f \rho_{sf} \\ & - \frac{\gamma}{2\pi^2} \sum_f \int_{k_{Ff}}^\Lambda dk k^2 (k^2 + M_f^2)^{1/2} - 2G_V \Phi^2 \sum_f \rho_f^2 \\ & + \mathcal{U}(\rho_{(u,d,s)}, \rho_{s(u,d,s)}, \Phi) - \Omega_{\text{vac}}, \quad (8) \end{aligned}$$

with the constant $\Omega_{\text{vac}} = -P_{\text{vac}}$ is added to ensure $P_{\text{PNJL0}} = \mathcal{E}_{\text{PNJL0}} = 0$ in vacuum. In these equations, one has quark masses and condensates written as

$$M_f = m_f - 2\mathcal{G}_s(G_s, \Phi)\rho_{sf} - 2\mathcal{K}(K, \Phi) \prod_{f' \neq f} \rho_{sf'}, \quad (9)$$

and

$$\rho_{sf} = -\frac{\gamma M_f}{2\pi^2} \int_{k_{Ff}}^\Lambda \frac{dk k^2}{(k^2 + M_f^2)^{1/2}}, \quad (10)$$

with $\rho_f = (\gamma/6\pi^2)k_{Ff}^3$ and $\gamma = N_s \times N_c = 6$ (degeneracy factor given in terms of spin, $N_s = 2$, and color, $N_c = 3$, numbers). Λ is the cutoff parameter and m_f is the current quark mass. The chemical potential of each quark reads

$$\mu_f = (k_{Ff}^2 + M_f^2)^{1/2} + 2\mathcal{G}_V(G_V, \Phi)\rho_f. \quad (11)$$

Finally, the new Polyakov potential, that is not vanishing at $T = 0$, is defined here as

$$\mathcal{U}(\rho_{(u,d,s)}, \rho_{s(u,d,s)}, \Phi) = G_V \Phi^2 \sum_f \rho_f^2 - G_s \Phi^2 \sum_f \rho_{sf}^2 - 4K\Phi^2 \prod_f \rho_{sf} + a_3 T_0^4 \ln(1 - 6\Phi^2 + 8\Phi^3 - 3\Phi^4), \quad (12)$$

for $T_0 = 190$ MeV. The last term in Eq. (12) ensures nonzero solutions for the traced Polyakov loop and also limits this quantity to the range of $0 < \Phi < 1$. In order to determine values for the quark condensates and for the traced Polyakov loop, it is needed to solve, simultaneously, Eqs. (9) and (10) in a self-consistent way, along with the condition of

$$\frac{\partial \Omega_{\text{PNJL0}}}{\partial \Phi} = 0, \quad (13)$$

where $\Omega_{\text{PNJL0}} = -P_{\text{PNJL0}}$.

The constants used in this work for the PNJL0 model are given by the Rehberg-Klevansky-Hufner parametrization, namely, $G_s = 3.67/\Lambda^2$, $K = -12.36/\Lambda^5$, $m_u = m_d = 5.5$ MeV, $m_s = 140.7$ MeV, and $\Lambda = 602.3$ MeV. The constants G_V and a_3 are the free parameters of the model. We verify in Sec. III how the variation of these quantities affect the meson properties.

For the calculation of the in medium single meson properties, we focus in two particular systems constructed from the PNL0 model. The first one consists of symmetric quark matter, for which the chemical potentials are equal, i.e., we take $\mu_u = \mu_d = \mu_s \equiv \mu$. The identification of the first order confinement/deconfinement phase transition can be clearly made by looking at the chemical potential dependence of the grand canonical potential density, as shown in Fig. 1a. This figure shows the signature of a first order phase transition, for which the traced Polyakov loop is the respective order parameter. As one can verify in Fig. 1b, Φ abruptly increases from $\Phi = 0$ to $\Phi > 0$ at the chemical potential related to the transition, in this case, $\mu = 529.5$ MeV. To determine the physical equation of state we use a Maxwell construction connecting the stable regions at both sides of the transition point. The appearing of nonvanishing solutions of Φ leads to the effects depicted in Fig. 2 related to the constituent quark masses, and quark Fermi momenta, respectively. It is clear that deconfinement leads to a substantial decreasing of M_s , leading the system to the direction of restoration of chiral symmetry. The Fermi momenta are also modified by Φ . Once again, the biggest change is observed for the strange flavor.

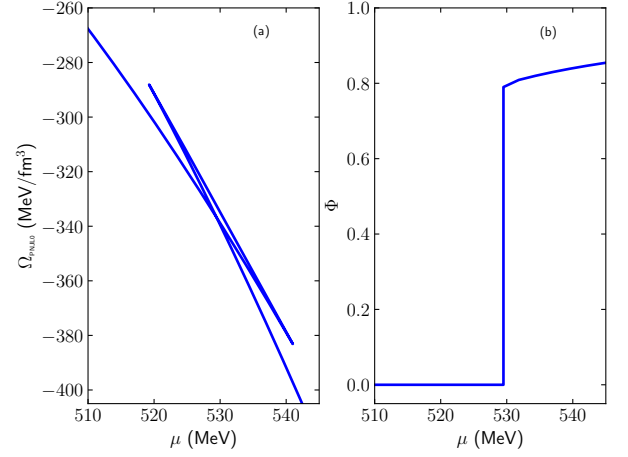


FIG. 1. (a) Ω_{PNJL0} and (b) Φ as a function of the common chemical potential for the PNJL0 model with $G_V/G_s = 0.2$, and $a_3 = -0.08$.

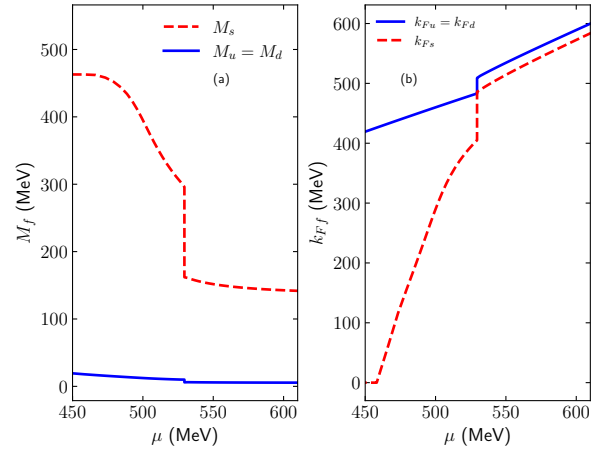


FIG. 2. (a) Constituent quark masses, and (b) quark Fermi momenta as a function of the common chemical potential for the PNJL0 model with $G_V/G_s = 0.2$, and $a_3 = -0.08$.

The second case analyzed here is the charge neutral system of quarks and leptons, namely, muons and massless electrons, in weak equilibrium. For this system, the relationship between the chemical potentials of quarks and leptons reads

$$\mu_u = \frac{\mu_B}{3} - \frac{2}{3}\mu_e, \quad (14)$$

$$\mu_d = \mu_s = \frac{\mu_B}{3} + \frac{1}{3}\mu_e, \quad (15)$$

$$\mu_e = \mu_\mu \quad (16)$$

where the indexes e and μ refer to electrons and muons, respectively. The baryonic chemical potential is given by μ_B . The charge neutrality of the system leads to

$$\frac{2}{3}\rho_u - \frac{1}{3}\rho_d - \frac{1}{3}\rho_s = \frac{\mu_e^3}{3\pi^2} + \frac{(\mu_\mu^2 - m_\mu^2)^{3/2}}{3\pi^2}, \quad (17)$$

with $m_\mu = 105.7$ MeV. For this system, we apply the same method performed in Ref. [20], namely, a hadron-quark phase transition using the PNJL0 model for the quark sector. For the hadronic side, we use a density-dependent model described the Lagrangian density given by

$$\begin{aligned} \mathcal{L}_{\text{HAD}} = & \bar{\psi}(i\gamma^\mu\partial_\mu - M)\psi + \Gamma_\sigma(\rho)\sigma\bar{\psi}\psi - \Gamma_\omega(\rho)\bar{\psi}\gamma^\mu\omega_\mu\psi \\ & - \frac{\Gamma_\rho(\rho)}{2}\bar{\psi}\gamma^\mu\vec{\rho}_\mu\vec{\tau}\psi + \Gamma_\delta(\rho)\bar{\psi}\vec{\delta}\vec{\tau}\psi + \frac{1}{2}(\partial^\mu\sigma\partial_\mu\sigma - m_\sigma^2\sigma^2) \\ & - \frac{1}{4}F^{\mu\nu}F_{\mu\nu} + \frac{1}{2}m_\omega^2\omega_\mu\omega^\mu - \frac{1}{4}\vec{B}^{\mu\nu}\vec{B}_{\mu\nu} + \frac{1}{2}m_\rho^2\vec{\rho}_\mu\vec{\rho}^\mu \\ & + \frac{1}{2}(\partial^\mu\vec{\delta}\partial_\mu\vec{\delta} - m_\delta^2\vec{\delta}^2), \end{aligned} \quad (18)$$

with

$$\Gamma_i(\rho) = \Gamma_i(\rho_0)a_i\frac{1+b_i(\rho/\rho_0+d_i)^2}{1+c_i(\rho/\rho_0+d_i)^2}, \quad (19)$$

for $i = \sigma, \omega$, and

$$\Gamma_i(\rho) = \Gamma_i(\rho_0)[a_ie^{-b_i(\rho/\rho_0-1)} - c_i(\rho/\rho_0 - d_i)]. \quad (20)$$

for $i = \rho, \delta$. ψ is the nucleon field and σ , ω^μ , $\vec{\rho}_\mu$, and $\vec{\delta}$ are the scalar, vector, isovector-vector, and isovector-scalar fields, respectively. The antisymmetric tensors $F_{\mu\nu}$ and $\vec{B}_{\mu\nu}$ are defined as $F_{\mu\nu} = \partial_\nu\omega_\mu - \partial_\mu\omega_\nu$ and $\vec{B}_{\mu\nu} = \partial_\nu\vec{\rho}_\mu - \partial_\mu\vec{\rho}_\nu$. Nucleon rest mass, and mesons masses are given by M_{nuc} , m_σ , m_ω , m_ρ , and m_δ .

The mean-field approximation is used once again in order to compute energy density and pressure of the model, namely,

$$\begin{aligned} \mathcal{E}_{\text{HAD}} = & \frac{1}{2}m_\sigma^2\sigma^2 - \frac{1}{2}m_\omega^2\omega_0^2 - \frac{1}{2}m_\rho^2\vec{\rho}_{0(3)}^2 + \frac{1}{2}m_\delta^2\delta_{(3)}^2 \\ & + \frac{\Gamma_\rho(\rho)}{2}\bar{\rho}_{0(3)}\rho_3 + \frac{1}{\pi^2}\int_0^{k_{Fp}} dk k^2(k^2 + M_p^{*2})^{1/2} \\ & + \Gamma_\omega(\rho)\omega_0\rho + \frac{1}{\pi^2}\int_0^{k_{Fn}} dk k^2(k^2 + M_n^{*2})^{1/2} \end{aligned} \quad (21)$$

and

$$\begin{aligned} P_{\text{HAD}} = & \rho\Sigma_R(\rho) - \frac{1}{2}m_\sigma^2\sigma^2 + \frac{1}{2}m_\omega^2\omega_0^2 + \frac{1}{2}m_\rho^2\vec{\rho}_{0(3)}^2 \\ & - \frac{1}{2}m_\delta^2\delta_{(3)}^2 + \frac{1}{3\pi^2}\int_0^{k_{Fp}} \frac{dk k^4}{(k^2 + M_p^{*2})^{1/2}} \\ & + \frac{1}{3\pi^2}\int_0^{k_{Fn}} \frac{dk k^4}{(k^2 + M_n^{*2})^{1/2}} \end{aligned} \quad (22)$$

with

$$\begin{aligned} \Sigma_R(\rho) = & \frac{\partial\Gamma_\omega}{\partial\rho}\omega_0\rho + \frac{1}{2}\frac{\partial\Gamma_\rho}{\partial\rho}\bar{\rho}_{0(3)}\rho_3 - \frac{\partial\Gamma_\sigma}{\partial\rho}\sigma\rho_s \\ & - \frac{\partial\Gamma_\delta}{\partial\rho}\delta_{(3)}\rho_{s3}, \end{aligned} \quad (23)$$

being the rearrangement term. The total scalar density is

$$\begin{aligned} \rho_s = & \rho_{sp} + \rho_{sn} \\ = & \frac{M^*}{\pi^2}\left[\int_0^{k_{Fp}} \frac{dk k^2}{\sqrt{k^2 + M_p^{*2}}} + \int_0^{k_{Fn}} \frac{dk k^2}{\sqrt{k^2 + M_n^{*2}}}\right], \end{aligned} \quad (24)$$

with $\rho_3 = \rho_p - \rho_n$, and $\rho_{p,n} = k_{F_{p,n}}^3/3\pi^2$. The fields are obtained as $\sigma = \Gamma_\sigma(\rho)\rho_s/m_\sigma^2$, $\omega_0 = \Gamma_\omega(\rho)\rho/m_\omega^2$, $\bar{\rho}_{0(3)} = \Gamma_\rho(\rho)\rho_3/2m_\rho^2$, and $\delta_{(3)} = \Gamma_\delta(\rho)\rho_{s3}/m_\delta^2$ with $\rho_{s3} = \rho_{sp} - \rho_{sn}$. Finally, the nucleon effective masses are

$$M_{p,n}^* = M_{\text{nuc}} - \Gamma_\sigma(\rho)\sigma \pm \Gamma_\delta(\rho)\delta_{(3)} \quad (25)$$

with $-(+)$ for protons (neutrons). The parametrization of the density dependent model used here is the DDH δ one [43–45].

In the case of beta equilibrated matter, the conditions that need to be satisfied in the hadronic side are the following: $\rho_p - \rho_e = \rho_\mu$ and $\mu_n - \mu_p = \mu_e = \mu_\mu$. In this case, the baryonic chemical potential is equal to the neutron chemical potential ($\mu_B = \mu_n$).

One way to perform the hadron-quark phase transition is through the Maxwell construction between the DDH δ model and the PNJL0 one. In this case, pressure and chemical potential of both phases are forced to be equal. The implementation of such an approach is displayed in Fig. 3. The total pressure is given by $P_t = P_{\text{HAD}} + P_{\text{lep}}$

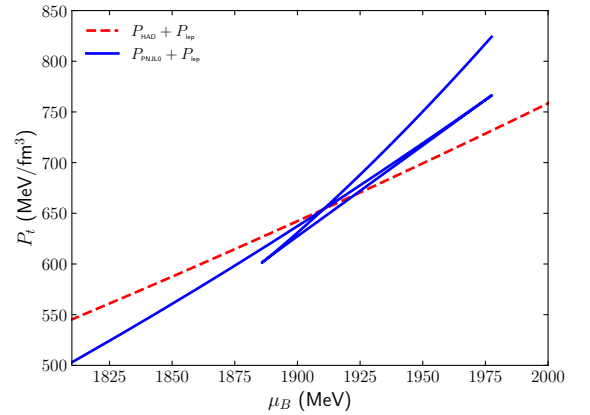


FIG. 3. Total pressure of beta equilibrated matter as a function of μ_B . For the PNJL0 model we take $G_V/G_s = 0.5$, and $a_3 = -0.458$.

in the dashed curve, and by $P_t = P_{\text{PNJL0}} + P_{\text{lep}}$ in the solid one, with P_{lep} being the sum of the electron and muon pressures. As in Ref. [20], we take the value of a_3 in the PNJL0 model that makes the hadron-quark phase transition coincide with the confinement/deconfinement one. The full curve in this case is formed by the dashed one from $\mu_B < \mu_{Bc}$, and by the solid one in the range of $\mu_B > \mu_{Bc}$. One has $\mu_{Bc} = 1910.4$ MeV for the parameter set used to construct this figure.

III. IN MEDIUM PROPERTIES OF THE PSEUDO-SCALAR MESONS

In this section we summarize the theoretical foundations of the single meson properties evaluated in the next sections. We are considering different frameworks, namely, within the PNJL0 model the mesons emerge as a quasiparticle of the quark-antiquark interaction. In the hadronic model, instead, the mesons are preexisting degrees of freedom which are dressed by their interaction with baryons. However, both situations are non-perturbative and are solved by summing a given diagram to all orders in a self-consistent approach. We consider here the lightest pseudoscalar meson nonet at zero temperature and for a density regime around the deconfinement phase transition.

A. Quark model

The mesonic modes have been studied in the SU(3) NJL model from long time ago [46] and developed subsequently [47, 48] even in the extended PNJL model at finite temperature [6]. For this purpose, the specific channel responsible for the excitation of a given mesonic mode is diagrammatically summed to all orders to build the polarization insertion $\Pi(p)$ within a random phase approximation (RPA). To accomplish this strategy, the contribution coming from the determinant in Eq. (1) must be rendered into an effective four quarks coupling by contracting $\bar{q}q$ pairs. In this approach the interaction giving rise to the meson modes is

$$\begin{aligned} & \sum_{a=0}^8 \left[L_a (\bar{q} \lambda^a q)^2 + K_a (\bar{q} i \gamma_5 \lambda^a q)^2 \right] \\ & + \sum_{a,b=0,3,8} (1 - \delta_{a,b}) [L_{ab} \bar{q} \lambda^a q \bar{q} \lambda^b q \\ & + K_{ab} \bar{q} i \gamma_5 \lambda^a q \bar{q} i \gamma_5 \lambda^b q]. \end{aligned} \quad (26)$$

The effective coupling constants are given by

$$K_0 = \mathcal{G}_s/2 - (\rho_{su} + \rho_{sd} + \rho_{ss})\mathcal{K}/3, \quad (27)$$

$$K_1 = K_2 = K_3 = (\mathcal{G}_s - \rho_{ss}\mathcal{K})/2, \quad (28)$$

$$K_4 = K_5 = (\mathcal{G}_s - \rho_{sd}\mathcal{K})/2, \quad (29)$$

$$K_6 = K_7 = (\mathcal{G}_s - \rho_{su}\mathcal{K})/2, \quad (30)$$

$$K_8 = \mathcal{G}_s/2 - (2\rho_{su} + 2\rho_{sd} - \rho_{ss})\mathcal{K}/6, \quad (31)$$

$$K_{03} = K_{30} = (\rho_{sd} - \rho_{su})\mathcal{K}/\sqrt{24}, \quad (32)$$

$$K_{08} = K_{80} = (\rho_{su} + \rho_{sd} - 2\rho_{ss})\mathcal{K}/\sqrt{72}, \quad (33)$$

$$K_{38} = K_{83} = (\rho_{su} - \rho_{sd})\mathcal{K}/\sqrt{12}. \quad (34)$$

The remaining ones L_a , L_{ab} participate only of the scalar meson construction and will not be used in the present calculations. It must be noted that for $\rho_{su} = \rho_{sd}$ we have $K_{38} = K_{30} = 0$ and the sector 3 decouples from the 0-8, that is the neutral pion becomes independent of the η - η' mesons. Since the sector 0-3-8 is generally coupled, the calculations are performed in two different instances. The charged pions and kaons properties are evaluated independently, while the π^0 , η , and η' are solved together.

The polarization insertion connecting states a and b is given by

$$\begin{aligned} i\Pi_{ab}(p) &= \\ &= N_c \sum_{j,k} \lambda_{jk}^a \lambda_{kj}^b \int \frac{d^4 q}{(2\pi)^4} \text{Tr} \{ i \gamma_5 G_j(q) i \gamma_5 G_k(p-q) \} \end{aligned} \quad (35)$$

which can be projected onto physical meson states as

$$\begin{aligned} i\Pi_a(p) &= \\ &= N_c \sum_{j,k} T_{jk}^a T_{kj}^a \int \frac{d^4 q}{(2\pi)^4} \text{Tr} \{ i \gamma_5 G_j(q) i \gamma_5 G_k(p-q) \} \end{aligned} \quad (36)$$

where $T^a = (\lambda_1 \pm i \lambda_2)/\sqrt{2}$ for $a = \pi^\pm$, $T^a = (\lambda_6 \pm i \lambda_7)/\sqrt{2}$ for $a = K^0$ (upper sign) or $a = \bar{K}^0$ (lower sign), and finally $T^a = (\lambda_4 \pm i \lambda_5)/\sqrt{2}$ for $a = K^\pm$.

The propagator $G_j(p)$ of the quark of flavor j in a real time formulation of the thermal field theory is written in the mean field approach as

$$\begin{aligned} G_j(p) &= \\ &= (\not{p} + M_j) \left[\frac{1}{\tilde{p}^2 - M_j^2 + i\varepsilon} + 2i\pi \Theta(\mu_j - \tilde{p}_0) n_F(\tilde{p}_0) \right] \end{aligned} \quad (37)$$

where $\tilde{p}_\nu = (p_0 - 2\mathcal{G}_V \rho_j, \mathbf{p})$ and n_F is the Fermi occupation number. We use the same cutoff Λ to deal with the divergent contributions coming from the Dirac sea. The explicit result for the integral in Eq. (35) is given in the case $\mathbf{p} = 0$ by

$$\int \frac{d^4 q}{(2\pi)^4} \text{Tr} \{i \gamma_5 G_j(q) i \gamma_5 G_l(p-q)\} = -\frac{\rho_{sj}}{M_j} - \frac{\rho_{sl}}{M_l} + \frac{N_c}{2\pi^2} \frac{\tilde{p}_0^2 - (M_j - M_l)^2}{\tilde{p}_0} \\ \times \left[k_{Fl} - k_{Fj} + C_j \ln \left(\frac{k_{Fj} + E_{Fj}}{\Lambda + E_{\Lambda j}} \right) - C_l \ln \left(\frac{k_{Fl} + E_{Fl}}{\Lambda + E_{\Lambda l}} \right) + W (F_j - F_l) \right] \quad (38)$$

where

$$F_i = \begin{cases} \arctan(k_{Fi}/W) - \arctan(x_i) + \arctan(y_i), & C_i^2 - M_i^2 < 0 \\ \frac{1}{2} \ln \left| \frac{1-x_i}{1+x_i} \frac{1-k_{Fi}/W}{1+k_{Fi}/W} \right| - \ln \left| \frac{1-y_i}{1+y_i} \right|, & C_i^2 - M_i^2 > 0 \end{cases}$$

and $E_{Fi} = \sqrt{k_{Fi}^2 + M_i^2}$, $E_{\Lambda i} = \sqrt{\Lambda^2 + M_i^2}$, $C_j = (M_j^2 - M_j^2 - \tilde{p}_0^2)/2\tilde{p}_0$, $C_l = C_j + \tilde{p}_0$, $W = \sqrt{|C_j^2 - M_j^2|} = \sqrt{|C_l^2 - M_l^2|}$, $x_i = C_i k_{Fi}/W E_{Fi}$, and $y_i = C_i \Lambda/W E_{\Lambda i}$. The meson polarizations can have an imaginary part under certain conditions which will be discussed in Sec. IV, the equation above shows only the real part.

The in medium meson mass m_a is obtained as the solution of the equation [47]

$$0 = 1 - 4K_a \Pi_a(p_0 = m_a, \mathbf{p} = 0), \quad (39)$$

in which the coupling must be chosen as $K_a = K_1$ for π^\pm , $K_a = K_4$ for K^\pm , and $K_a = K_6$ for the neutral kaons. Furthermore, the effective meson-quark-antiquark couplings $G_{\alpha q}$ can be identified from a pole approximation as

$$G_{\alpha q}^{-2} = \frac{1}{m} \left. \frac{\partial \Pi_\alpha}{\partial p_0} \right|_{p_0=m}. \quad (40)$$

In the case of the coupled $\pi^0 \eta \eta'$ sector, the calculations must be done in a matrix framework by introducing the quantities

$$\mathbb{K} = \begin{pmatrix} K_3 & K_{30} & K_{38} \\ K_{03} & K_0 & K_{08} \\ K_{83} & K_{80} & K_8 \end{pmatrix}, \quad \mathbb{P} = \begin{pmatrix} \Pi_{33} & \Pi_{30} & \Pi_{38} \\ \Pi_{03} & \Pi_{00} & \Pi_{08} \\ \Pi_{83} & \Pi_{80} & \Pi_{88} \end{pmatrix} \quad (41)$$

and $\mathbb{M}^{-1} = \mathbb{K}^{-1} - \mathbb{P}$. The last matrix has a set of eigenvalues $\nu_i(p)$, $i = 1 - 3$ which are used to define the mass m through the solutions of $0 = \nu_i(p_0 = m, \mathbf{p} = 0)$ for the π^0 ($i = 1$), η ($i = 2$), and η' ($i = 3$).

B. Hadronic model

The study of the meson properties in a dense hadronic environment is a longstanding issue [1]. The importance of the variation of the constitutive properties of the lightest mesons has been emphasized in different situations. In nuclear physics the role of the pion [49], correlated pion exchange [50] and σ meson [51], have been remarked. For the description of medium and large matter densities the use of scalar and vector fields $\sigma, \omega, \bar{\rho}, \delta$ has become a

standard procedure [52]. The possibility of meson condensation in neutron stars has intensified the study of the kaon properties [12, 33, 53, 54], while the analysis of exotic nuclei has regarded the interaction between nucleons and π, K , and η mesons [26, 28].

A large number of such investigations are based on the $SU(3) \times SU(3)$ chiral Lagrangian, keeping a low order expansion in inverse powers of the chiral symmetry breaking scale. As a consequence the range of applicability is expected to extend over a density range of several times the normal nuclear density $\rho_0 = 0.16 \text{ fm}^{-3}$. In addition, there are significant research using effective models founded on semi-phenomenological considerations.

In a preceding publication [20], a composition of the PNJL0 model and the hadronic model with density dependent couplings DDH δ has been done in order to match the threshold of the deconfinement transition. With the aim to continue this approach we extend here the DDH δ model by including additional terms which consider the role of π, K , and η mesons. In the absence of pseudoscalar meson condensation, these new contributions do not modify the Euler equations used to obtain the results shown in Section II. Thus, we add to \mathcal{L}_{HAD} the sum of three independent contributions, namely

$$\mathcal{L} = \mathcal{L}_\pi + \mathcal{L}_K + \mathcal{L}_\eta, \quad (42)$$

which have been selected for their ability to describe the main features of the mesons in a dense medium in a concise formulation.

The first term is the Weinberg model of the pion-nucleon interaction [55], proposed for low energy pion-nucleon scattering and satisfies the Goldberger-Treiman relation. It reads as

$$\mathcal{L}_\pi = \frac{g_A}{2f_\pi} \bar{\Psi} \gamma^\mu \gamma^5 \boldsymbol{\tau} \cdot \partial_\mu \boldsymbol{\pi} \Psi - \frac{1}{f_\pi^2} \bar{\Psi} \boldsymbol{\tau} \Psi \cdot (\boldsymbol{\pi} \times \partial_\mu \boldsymbol{\pi}) \quad (43)$$

The bi-spinor Ψ has the proton and neutron components $\Psi_1 = \psi_p$, $\Psi_2 = \psi_n$. The second term in the equation above is known as the Weinberg-Tomozawa interaction and contributes at lowest order only to the charged pion polarization. The first term contributes at the second order with a bubble diagram included in a RPA. Thus,

one obtains

$$i\Pi_\alpha(p) = i\Pi_\alpha^{\text{OPE}}(p) + i\Pi_\alpha^{\text{WT}}(p) \quad (44)$$

$$i\Pi_\alpha^{\text{OPE}}(p) = \left(\frac{g_A}{2f_\pi}\right)^2 p_\mu p_\nu \times \\ \times \sum_{a,b=1,2} \xi_\alpha \int \frac{d^4 q}{(2\pi)^4} \text{Tr} \left[\gamma^\mu \gamma_5 G^{(a)}(q) \gamma^\nu \gamma_5 G^{(b)}(q-p) \right] \quad (45)$$

$$i\Pi_\alpha^{\text{WT}}(p) = -\frac{\epsilon_\alpha}{f_\pi^2} p_\mu \sum_{c=1,2} \tau_3^{cc} \int \frac{d^4 q}{(2\pi)^4} \text{Tr} \left[\gamma^\mu G^{(c)}(q) \right]. \quad (46)$$

The index α discriminates the isotopic component, for the neutral pion is $\epsilon_\alpha = 0$, $\xi_\alpha = \delta_{a,b}$, for the π^- one

must take $\epsilon_\alpha = 1$, $\xi_\alpha = 2\delta_{a,2}\delta_{b,1}$ and finally for the π^+ is $\epsilon_\alpha = -1$, $\xi_\alpha = 2\delta_{a,1}\delta_{b,2}$. The nucleon propagators have, in a real time formulation of the thermal field theory, an expression similar to Eq. (37)

$$G^{(a)}(p) = (\not{p} + M_a^*) \left[\frac{1}{\tilde{p}^2 - M_a^{*2} + i\varepsilon} + 2i\pi \Theta(\mu_a - \tilde{p}_0) n_F(\tilde{p}_0) \right] \quad (47)$$

but with

$$\tilde{p}_\mu = \left(p_0 - \Gamma_\omega \omega_0 \mp \frac{\Gamma_\rho}{2} \rho_{0(3)} - \Sigma_{R,\mathbf{p}} \right). \quad (48)$$

The explicit formulae for these components are easily obtained as

$$\Pi_\alpha^{\text{OPE}}(p_0, \mathbf{p} = 0) = \left(\frac{g_A p_0}{2f_\pi \tilde{p}_0}\right)^2 \sum_{a,b=1,2} \xi_\alpha \left\{ \frac{1}{2} (M_a^{*2} - M_b^{*2}) \left(\frac{\rho_{sb}}{M_a^*} - \frac{\rho_{sa}}{M_b^*} \right) + \tilde{p}_0 (\rho_b - \rho_a) \right. \\ \left. + \left(\frac{M_a^* + M_b^*}{2\pi}\right)^2 \frac{(M_a^* - M_b^*)^2 - \tilde{p}_0^2}{\tilde{p}_0} \left[k_{Fb} - k_{Fa} + C_a \ln \left(\frac{k_{Fa} + E_{Fa}}{M_a^*} \right) \right. \right. \\ \left. \left. - C_b \ln \left(\frac{k_{Fb} + E_{Fb}}{M_b^*} \right) + W (F_b - F_a) \right] \right\}, \quad (49)$$

$$\Pi_\alpha^{\text{WT}}(p_0, \mathbf{p} = 0) = \frac{\epsilon_\alpha}{2f_\pi^2} (\rho_p - \rho_n). \quad (50)$$

Here only the real part of Π^{OPE} is shown, while the effects of the imaginary term are discussed in section IV. As usually done in this framework, the divergent contribution coming from the Dirac sea has been neglected. The following definitions have been used

$$F_c = \begin{cases} \arctan(k_{Fc}/W) + \arctan(x_c), & C_k^2 - M_k^{*2} < 0 \\ \frac{1}{2} \ln \left| \frac{1+x_c}{1-x_c} \frac{1-k_{Fc}/W}{1+k_{Fc}/W} \right|, & C_k^2 - M_k^{*2} > 0 \end{cases},$$

together with $C_b = (M_a^{*2} - M_b^{*2} + \tilde{p}_0^2)/2\tilde{p}_0$, $C_a = C_b -$

\tilde{p}_0 , $W = \sqrt{|C_b^2 - M_b^{*2}|}$, $E_{Fc} = \sqrt{k_{Fc}^2 + M_c^{*2}}$, and $x_c = C_c k_{Fc}/W E_{Fc}$.

The second term in Eq. (42) corresponds to the kaon-nucleon interaction and is taken from [35]. The model is based on a SU(3) chiral symmetric Lagrangian plus symmetry breaking terms respecting the partial conservation of the axial current, taken in the MFA [56]. The relevant terms for our calculations are

$$\mathcal{L}_K = \frac{-i}{4f_K^2} \left[(2\bar{\psi}_1 \gamma^\mu \psi_1 + \bar{\psi}_2 \gamma^\mu \psi_2) (K^- \partial_\mu K^+ - K^+ \partial_\mu K^-) + (\bar{\psi}_1 \gamma^\mu \psi_1 + 2\bar{\psi}_2 \gamma^\mu \psi_2) (\bar{K}^0 \partial_\mu K^0 - K^0 \partial_\mu \bar{K}^0) \right] \\ + \frac{m_K^2}{2f_K} [(\sigma + \delta) K^+ K^- + (\sigma - \delta) K^0 \bar{K}^0] - \frac{1}{f_K} [(\sigma + \delta) \partial_\mu K^+ \partial^\mu K^- + (\sigma - \delta) \partial_\mu K^0 \partial^\mu \bar{K}^0] \\ + \frac{d_1}{2f_K^2} (\bar{\psi}_1 \psi_1 + 2\bar{\psi}_2 \psi_2) \partial_\mu K^0 \partial^\mu \bar{K}^0 + \frac{d_2}{2f_K^2} (\bar{\psi}_1 \psi_1 \partial_\mu K^+ \partial^\mu K^- + \bar{\psi}_2 \psi_2 \partial_\mu K^0 \partial^\mu \bar{K}^0). \quad (51)$$

Treating the first order contribution to the kaon polar-

ization, the following results are obtained [35]

$$\Pi_{K^\pm}(p) = \mp \frac{p_0}{2f_K^2} (2\rho_p + \rho_n) + \frac{m_K^2}{2f_K} (\sigma + \delta) + (p_0^2 - \mathbf{p}^2) \times \\ \times \left[-\frac{\sigma + \delta}{f_K} + \frac{d_1}{2f_K^2} (\rho_{sp} + \rho_{sn}) + \frac{d_2}{2f_K^2} \rho_{sp} \right], \quad (52)$$

and

$$\Pi_{K^0}(p) = \mp \frac{p_0}{2f_K^2} (\rho_p + 2\rho_n) + \frac{m_K^2}{2f_K} (\sigma - \delta) + (p_0^2 - \mathbf{p}^2) \times \left[-\frac{\sigma - \delta}{f_K} + \frac{d_1}{2f_K^2} (\rho_{sp} + \rho_{sn}) + \frac{d_2}{2f_K^2} \rho_{sn} \right]. \quad (53)$$

In the last equation the upper (lower) sign corresponds to the K^0 (\bar{K}^0).

In order to match the prescriptions given in [35], we have identified the fluctuations around the vacuum values of the σ and δ fields with the mean field values described in Sec. II. The numerical values of the parameters are $f_K = 122$ MeV, $d_1 = 2.5/m_K$, and $d_2 = 0.72/m_K$.

The last term of Eq. (42) stands for the nucleon-eta coupling, which we chose as proposed in [37]. It results from a low momentum approach to the s-wave ηN scattering starting from the chiral Lagrangian, and is given by

$$\mathcal{L}_\eta = \frac{1}{2f_\pi^2} \bar{\Psi} (\Sigma_{\eta N} \eta^2 + \kappa \partial_\mu \eta \partial^\mu \eta) \Psi. \quad (54)$$

The fact that this interaction is quadratic in the meson field can be used, as in the kaon case, to correct its propagator with a first order diagram. The polarization insertion obtained in such approach is

$$\Pi_\eta(p) = -\frac{1}{f_\pi^2} (\Sigma_{\eta N} + \kappa p_\mu p^\mu) (\rho_{sp} + \rho_{sn}), \quad (55)$$

and the model parameters are fixed as $\Sigma_{\eta N} = 283$ MeV and $\kappa = 0.4$. For each meson described by the interactions of Eq. (42), the in-medium effective mass m_X^* of the $X = \pi, K, \eta$ meson is determined by solving the equation

$$0 = m_X^{*2} - m_X^2 - \Pi_X(p_0 = m_X^*, \mathbf{p} = 0), \quad (56)$$

where m_X represents the in-vacuum mass.

IV. RESULTS AND DISCUSSION

The total baryon number is a conserved charge of the strong interaction, therefore if ρ_B is used for the baryon number per unit volume and ρ_q for the particle number density for each flavor, then the local constraint $\rho_B = \sum_q \rho_q/3$ always holds in quark matter. In the following we show and discuss the results for the meson properties under two different flavor compositions of homogeneous dense matter. In the first case we consider independent flavor conservation, so that a chemical potential μ_q is assigned to each flavor present in the Fermi sea, and the complementary condition $\mu_u = \mu_d = \mu_s$ is imposed. This configuration is named as symmetric flavor matter (SFM), although it does not imply equal proportions of all the flavors. In particular, the strange quark could be absent if $M_s > \mu_{u,d}$, circumstantially it

would present a threshold point where this inequality is reversed. In the second case we focus on matter under local electric neutrality, with the possible contribution of electrons, a situation denoted in the following as stellar matter (SM).

The PNJL0 and NJL results coincide in the low density regime, where $\Phi = 0$ and there exist a well known instability for quark matter. It has been identified as a partial restoration of the chiral symmetry, which for low values of the parameter G_V/G_s gives rise to a first order phase transition. As G_V/G_s is raised, the transition becomes a smooth crossover. The behavior of the pseudoscalar mesons within this domain has been studied for instance in [4, 48, 57], therefore, we do not consider here its explicit analysis.

We start this discussion considering SFM in the PNJL0 model. The results for the pions are displayed in Fig. 4. It is possible to see gaps in M_π and $G_{\pi q}$ due to the

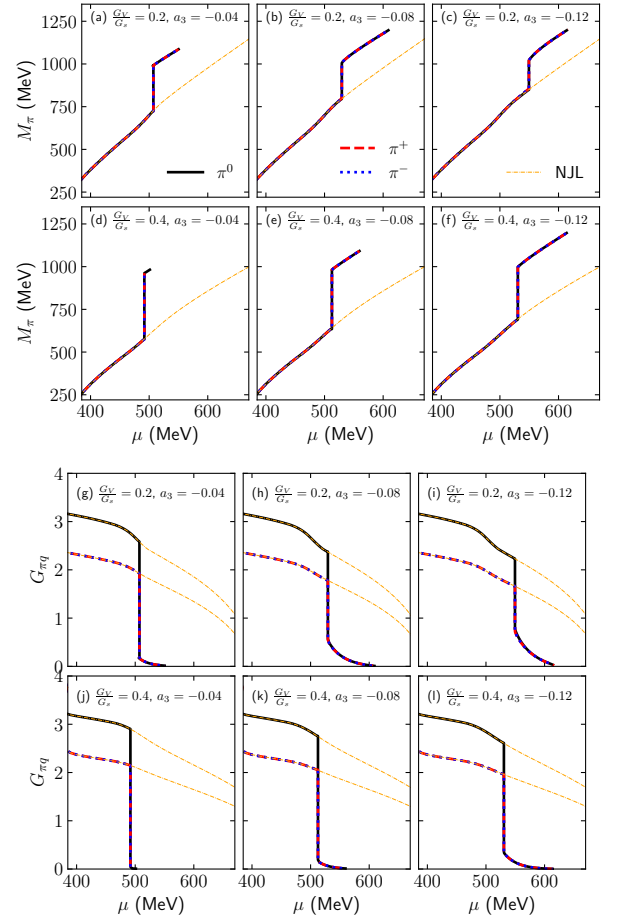


FIG. 4. Pion masses, and pion-quark couplings obtained from the PNJL0 model (symmetric matter case) for different parametrizations, namely, $(G_V/G_s, a_3)$ given by (a,g) (0.2, -0.04), (b,h) (0.2, -0.08), (c,i) (0.2, -0.12), (d,j) (0.4, -0.04), (e,k) (0.4, -0.08), and (f,l) (0.4, -0.12). Dotted-dashed lines: NJL model results.

transition to the deconfined phase that takes place in

the PNJL0 model. This feature is present for different values of G_V and a_3 , taken as free parameters of the model. In the case of the pion masses, the appearance of nonzero solutions of the traced Polyakov loop induces a significant increase in M_π . The opposite happens for the pion-quark couplings, namely, an abrupt decrease occurs at the chemical potential in which the transition occurs. Because of the degeneracy in the light $u - d$ sector, all curves corresponding to the different isotopic components coalesce. An almost linear increase with the chemical potential is obtained for all the cases, and particularly at the deconfinement threshold such increase takes place discontinuously. The gap in the pion mass increase with both G_V and a_3 , and varies from 200 MeV to 380 MeV. At the transition point the pion is not longer a light excitation, since it is between 4-6 times heavier than at zero density. A measure of the interaction of the pion with its environment is given by $G_{\pi q}$, its effective coupling with the quark-antiquark pair, shown in the bottom panels of Fig. 4. It can be appreciated that the greater value of G_V stabilize the density dependence of the remnant interaction of the pions, at both sides of the transition. A drastic reduction of $G_{\pi q}$ at the transition point leads to a regime of almost non-interacting pions. An increase of $|a_3|$ attenuates this drop, as is more evident for the $G_V/G_s = 0.2$ case.

The variation of the kaon mass in the SFM is displayed in Fig. 5. The curves corresponding to \bar{K}^0 and K^- coincide as well as those for K^0 and K^+ do, because of the symmetry of the non-strange quarks. Within the pure NJL model the onset of the strange quark manifests by a slowing down of the increase of the masses M_{K^0} and M_{K^+} , in contrast with the quick variation of $M_{\bar{K}^0}$ and M_{K^-} with the chemical potential. The difference can be attributed to the fact that in the former case the strange quark enters as an antiquark and does not follow directly the sudden changes of the valence quarks. The strangeness onset takes place around $\mu \simeq 460$ MeV, which corresponds to a baryonic density $\rho_B/\rho_0 \simeq 4.3$ for $G_V/G_s = 0.2$ and $\rho_B/\rho_0 \simeq 3.7$ for $G_V/G_s = 0.4$. This feature contrasts with other calculations where the role of the valence strange quarks are neglected [48, 58]. The non-monotonous dependence of the masses of the kaons K^0 , K^+ extends to higher densities, and part of such behavior takes place within the instability region. Hence, it is partially suppressed by the Maxwell construction performed within the PNJL0. Since an increase of $|a_3|$ shifts the transition point towards higher densities, the cases with $a_3 = -0.12$ preserve more complete this pattern, caused by the strange quark in the NJL model. At the transition threshold a discontinuous increase of the masses of all the kaons happens in a different manner. The mass of the mesons with strangeness $S = 1$ experience a gap around 100 MeV, while the change is more abrupt for the $S = -1$ case, with a gap taking values from 200 MeV to 400 MeV approximately. This result is valid for all the parametrizations studied. Beyond that point, a linear increase follows with very similar values for

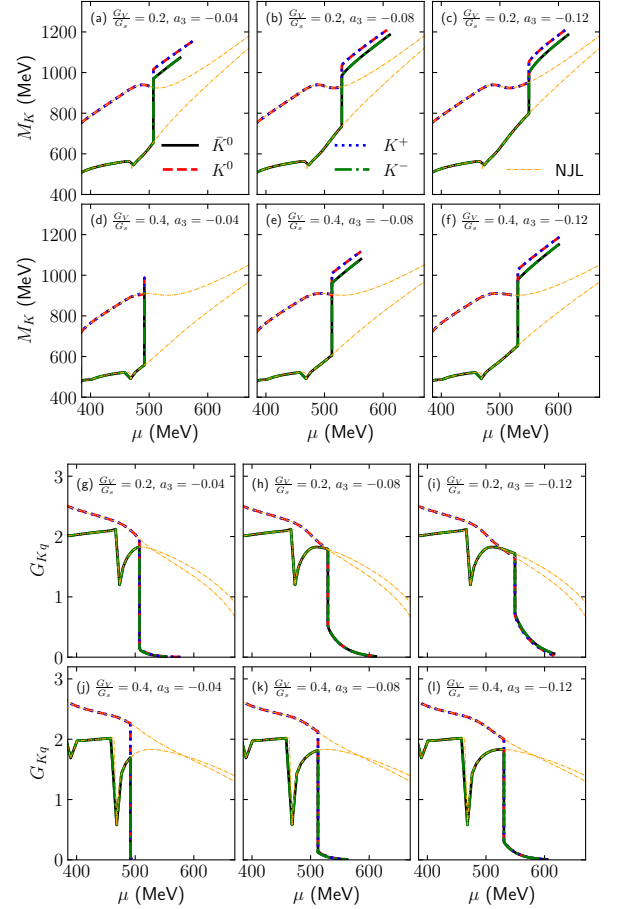


FIG. 5. Kaon masses, and kaon-quark couplings obtained from the PNJL0 model (symmetric matter case) for different parametrizations, namely, $(G_V/G_s, a_3)$ given by (a,g) (0.2, -0.04), (b,h) (0.2, -0.08), (c,i) (0.2, -0.12), (d,j) (0.4, -0.04), (e,k) (0.4, -0.08), and (f,l) (0.4, -0.12). Orange dotted-dashed lines: NJL model results.

all the isotopes and the masses are greater than 1 GeV.

The effective coupling of the kaon with a $q\bar{q}$ pair is shown in the lower panels of Fig. 5. As in the case of pions, one can distinguish the evolution from a phase of mesons interacting with its environment to a gas of quasi-free bosons. The activation of the valence strange quarks manifests by a sudden decrease of the effective coupling of the $S = -1$ kaons, followed by a similarly quick restoration of its previous value. This critical variation of G_{Kq} has been found for instance in [58], although in our calculations there is no a complete collapse but we have found multiple solutions at that point. With regard to the local minimum shown by the effective coupling in Figs. 5j, 5k, and 5l at μ slightly below 400 MeV, it can be identified as a threshold effect due to the fact that the meson excitation becomes a resonance [59].

The masses of the $\eta - \eta'$ system shown in Fig. 6 exhibits a similar variation as described for pions and kaons. The coincidence with the NJL results are extended to higher

densities as $|a_3|$ grows, and a discontinuous increment is experienced at the transition point followed by a linear increase with degenerate masses.

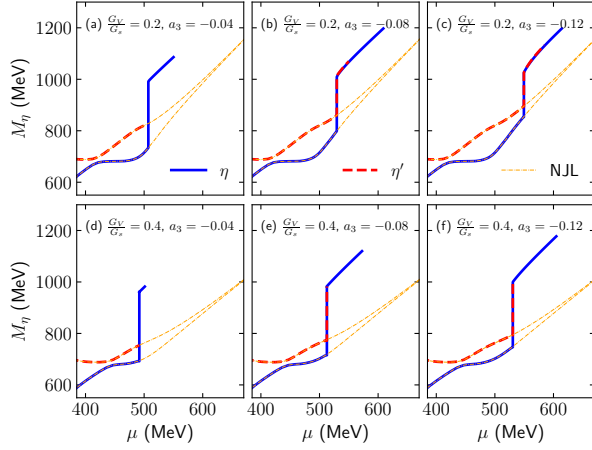


FIG. 6. η and η' masses obtained from the PNJL0 model (symmetric matter case) for different parametrizations, namely, $(G_V/G_s, a_3)$ given by (a) $(0.2, -0.04)$, (b) $(0.2, -0.08)$, (c) $(0.2, -0.12)$, (d) $(0.4, -0.04)$, (e) $(0.4, -0.08)$, and (f) $(0.4, -0.12)$. Orange dotted-dashed lines: NJL model results.

It must be pointed out that within our approach and using the specific parametrization shown in Fig. 6d, all the mesonic excitations are extinguished in the deconfined phase, since the solutions for the effective masses cease to exist.

The discussion of the imaginary part of the meson polarization is given in terms of the quantity $\tilde{m} = m - 2G_V(\rho_a - \rho_b)$, with a, b standing for the flavors of quark and antiquark composing the meson, and m is its in medium mass. Since near the transition point is $m \gg 2G_V(\rho_a - \rho_b)$ we consider in the following only the case $\tilde{m} > 0$. There are two sets of conditions for the arising of an imaginary part coming from the Dirac sea. The first one is composed by two simultaneous inequalities

$$0 < \tilde{m} \leq M_b - M_a, \quad (57)$$

$$\left[\tilde{m}^2 - (M_a + M_b)^2 \right] \left[\tilde{m}^2 - (M_a - M_b)^2 \right] < 4\Lambda^2 \tilde{m}^2. \quad (58)$$

Eventually, one must take $\Lambda \rightarrow \infty$. For the second set we have

$$\tilde{m} > M_a + M_b, \quad (59)$$

$$\left[\tilde{m}^2 - (M_a + M_b)^2 \right] \left[\tilde{m}^2 - (M_a - M_b)^2 \right] < 4\Lambda^2 \tilde{m}^2. \quad (60)$$

An instability could also arise from the Fermi sea, in which case we would have the same two sets of conditions but replacing Λ by p_{Fa} in Eq. (58) and by p_{Fb} in Eq. (60).

We have verified that the meson polarization insertions become complex in the deconfined phase, indicating that the mesonic excitations are unstable at extreme densities.

Now we focus on the results of the stellar matter case. For this purpose, we use here the same parameters sets studied in Ref. [20], i.e., parametrizations of the PNJL0 model given by (i) set I: $G_V/G_s = 0.15$, $a_3 = -0.052$; (ii) set II: $G_V/G_s = 0.25$, $a_3 = -0.135$; (iii) set III: $G_V/G_s = 0.35$, $a_3 = -0.241$; and (iv) set IV: $G_V/G_s = 0.5$, $a_3 = -0.458$. At the low density regime we have used the hadronic DDH δ model and both of them were connected through the Maxwell construction, in this case giving rise to a hadron-quark phase transition with the quark side composed by deconfined quarks, i.e., region in which $\Phi > 1$.

The behavior of the meson masses in SM is simpler, mainly because the confined phase is described by a hadronic model. The interaction between nucleons and pseudoscalar mesons is motivated by the chiral model [53], and corresponds to a low order approximation. Therefore it is adequate for a range of densities below $2\rho_0$, and extrapolations above such domain are highly speculative. Moreover, our results are obtained in a mean field approach excepting the pions which receive a special treatment due to its nature of lowest Goldstone boson. The loss of the symmetry in the light quark sector induces the splitting between the members of a given isomultiplet. However, beyond the deconfinement transition they become almost degenerate and unstable for all the considered cases.

The pion masses are shown in Fig. 7, for several parameter sets. As the increase of G_V implies an increase of

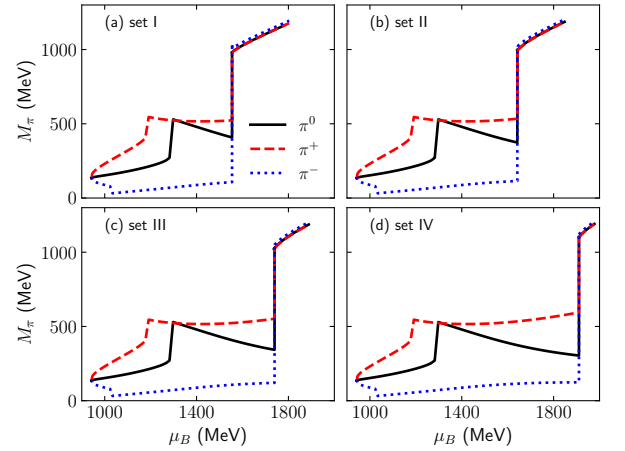


FIG. 7. Pion masses obtained from the PNJL0 model coupled to the DDH δ one (stellar matter case) for different parametrizations: (a) set I, (b) set II, (c) set III, and (d) set IV.

$|a_3|$, we find that, in agreement with the result stated in the SFM case, the confinement region extends to higher values of μ as G_V is increased. Furthermore, the mass gap at the transition point also increases with G_V . In the hadronic matter the masses of the multiplet are clearly

separated for densities above $\rho_0/2$, showing a smooth variation until a point of discontinuity. Beyond such points the pions can exist only as unstable excitations.

In regard of the kaons, there is a clear difference between the $S = 1$ and $S = -1$ components as can be seen in Fig. 8. In the first case, where u, d flavors enter as

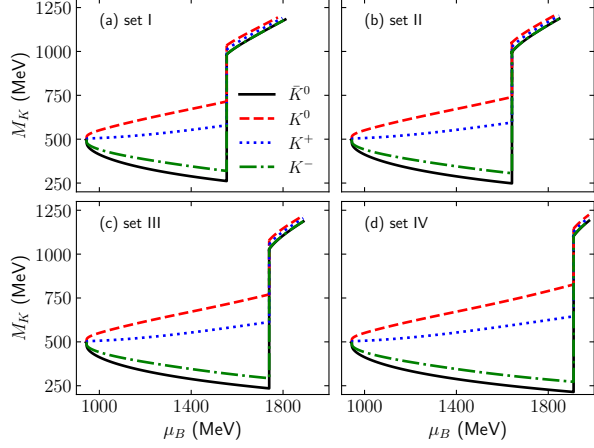


FIG. 8. Kaon masses obtained from the PNJL0 model coupled to the DDH δ one (stellar matter case) for different parametrizations: (a) set I, (b) set II, (c) set III, and (d) set IV.

antiparticles, a monotonous slight decrease with μ_B is obtained. In contrast, the masses of both K^+ and K^0 show an increasing behavior. These results are in qualitative agreement with those found by [35].

The η meson mass as function of the chemical potential is displayed in Fig. 9. It experiences a strong decrease

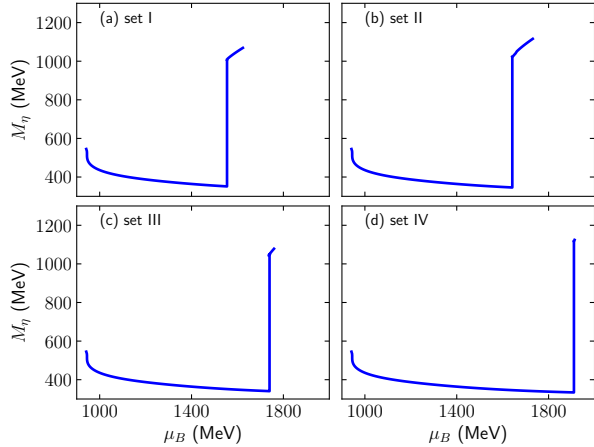


FIG. 9. η mass obtained from the PNJL0 model coupled to the DDH δ one (stellar matter case) for different parametrizations: (a) set I, (b) set II, (c) set III, and (d) set IV.

at very low densities in the hadronic environment, before reaching a slight decreasing slope. In the last regime the mass M_η experiences a strong discontinuity at the threshold.

Finally, for the sake of completeness, we present in Figs. 10-?? the mesons masses calculated exclusively from the PNJL0 model in SM as functions of the baryonic chemical potential μ_B . Although the models used to describe densities below the deconfinement threshold have dissimilar implementations, all of them are guided by the ideas of chiral symmetry. This is the motivation to make a daring contrast of the predictions for the in-medium meson masses given by the PNJL0 and by the effective hadronic models, paying special attention to the neighborhood of the transition point.

As the first comparison we consider the pion field in Figs. 10 and 7. Its effective mass has, within the domain

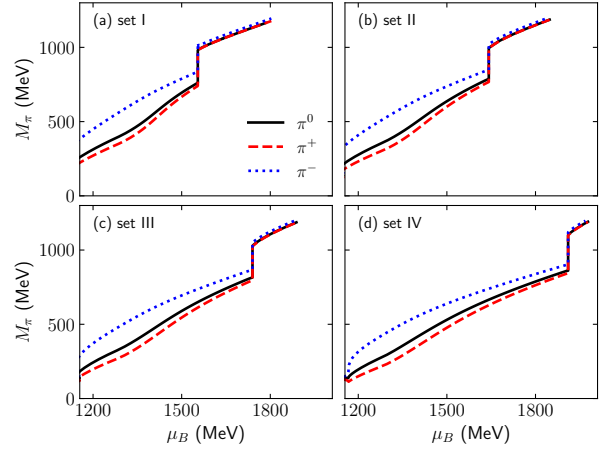


FIG. 10. Pion masses obtained from the PNJL0 model (stellar matter case) for different parametrizations: (a) set I, (b) set II, (c) set III, and (d) set IV.

$1050 \text{ MeV} \leq \mu_B < 1200 \text{ MeV}$, a similar increasing trend in both approaches. For μ_B slightly below 1200 MeV , corresponding to a baryon density around $2.8\rho_0$, the hadronic model shows a discontinuity in the π^+ mass, followed by a plateau. The value $m_\pi \simeq 500 \text{ MeV}$ taken at this point, marks the possible limit of applicability of the model. In contrast, the PNJL0 predicts a monotonous increase, as a consequence the mass gap at the transition point is comparatively reduced. We expect the physical behavior for $\mu_B > 1200 \text{ MeV}$ must lie between these qualitative descriptions. A similar conclusion holds for the π^0 case.

As the next step we analyze the kaon masses in Fig. 11. A contrast with the results shown in Fig. 8 evidences the smooth behavior, typical of the mean field approach, obtained with the hadronic model, while the output of the PNJL0, using a RPA, is more irregular. However, the monotonous increase of the masses of the $S = 1$ kaons is common for both calculations, but more pronounced in the latter case. For the $S = -1$ kaons, instead, these treatments give opposite behaviors. The main reason is the negative contribution of the Weinberg-Tomozawa term of the hadronic model [35] to the polarization of both kaons. Moreover, the slope of the masses of the

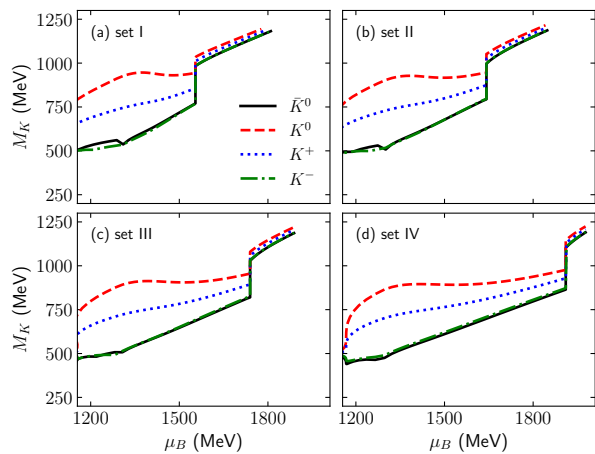


FIG. 11. Kaon masses obtained from the PNJL0 model (stellar matter case) for different parametrizations: (a) set I, (b) set II, (c) set III, and (d) set IV.

$S = -1$ kaons is increased in the PNJL0 after the onset of the strange quarks to the Fermi sea. In contrast, for the hadronic model there is no strange degree of freedom since we are considering nuclear matter. As for the pion masses, the faster increase with μ_B in the low density regime of the PNJL0 leads to a lesser discontinuity of the kaon masses at the deconfinement threshold.

To close this section we compare briefly the result for the η mass in the PNJL0, as shown in Fig. ??, with the predictions of the hadronic model. There is a clear opposition between the monotonous decrease found in the latter and the definitely increasing output of the PNJL0 model. It must be bear in mind that the treatment of the quark model includes the $\pi^0 - \eta - \eta'$ mixing which is significant as the $u - d$ symmetry is lost, as in fact occurs in the neutral and beta equilibrated matter. In the hadronic model, instead, this feature is disregarded and the parameter κ is determined by using the low-energy $\eta - N$ scattering data.

V. SUMMARY AND CONCLUDING REMARKS

In this work we focus on the calculation of masses and couplings related to the pseudoscalar π , K , and η mesons. For this purpose, we have used an effective three-flavor quark model studied in Ref. [20] (PNJL0 model) in which the phenomenology of the confinement/deconfinement phase transition at zero temperature is taken into account by means of the traced Polyakov loop, Φ . In this model, the strength of the scalar, vector, and 't Hooft channels are converted into Φ -dependent functions which vanish asymptotically in the deconfined region when $\Phi \rightarrow 1$. This approach leads to a typical first order phase transition, for which Φ is the order parameter, even at zero temperature regime. This is a feature that is not present in most of the PNJL models, that reduce

to the NJL one at $T = 0$ limit. As performed in Ref. [20], we consider the PNJL0 model in two different scenarios, both at $T = 0$. The first one takes into account the symmetric flavor matter (SFM), for which the quark chemical potentials are equal but with different flavors distributed in different proportions (the quark densities are different from each other). In the second case we focus on quark matter under beta equilibrium conditions, i.e., with local charge neutrality and chemical equilibrium. We named this scenario as the stellar matter case (SM). For the latter case we describe the hadron-quark phase transition by combining the PNJL0 model at the quark sector, and the relativistic density dependent model DDH δ at the hadronic side. The connection between both sectors is made from the Maxwell construction, namely equality of pressures and chemical potentials are imposed at the boundary of both phases.

The mesons properties were calculated through the random phase approximation, used in order to build the polarization insertion Π_a (related to the specific meson a). This quantity is used to extract the in-medium mesons masses as well as the effective meson-quark-antiquark couplings, in this case identified from a pole approximation. For the SFM scenario, Π_a is exclusively obtained from the PNJL0 model, from which Fermi momenta, constituent masses and Φ are used as input to solve Eqs (39) and (40). As a first result, we verified that, for the pions, the deconfined phase (nonzero solutions of Φ) induces a significant increase in their masses, and a drastic reduction in the pions-quark couplings indicating an almost free pions regime. The gap in the masses increase with the free parameters of the model, namely, the strength of the vector channel G_V , and the constant a_3 that regulates the magnitude of the Polyakov potential. For the sake of comparison, we shown that our results coincide with the NJL ones in the low chemical potential (or density) regime, region where the confinement takes place ($\Phi = 0$ solutions). The differences arise exactly at the chemical potential where the $\Phi > 0$ solutions appear. At this point, the almost linear increase exhibited at the confined region presents a discontinuity. Concerning the kaons, we verified that the \bar{K}_0 and K^- coincide as well as those for K_0 and K^+ due to the symmetry of the non-strange quarks. The non-monotonous dependence of their masses in the NJL model is partially suppressed in the case of the PNJL0 model. At the critical chemical potential, value at which it is verified the beginning of the nonzero Φ solutions, it is observed different behaviors for each kaon. For those with $S = 1$, the mass gap exhibited is around 100 MeV while the $S = -1$ kaons present a gap between 200 MeV and 400 MeV approximately. Concerning the effective coupling for the kaons, we observe a similar pattern in comparison with the pions case. It is possible to clearly distinguish a phase of interacting kaons from the one in which the system reaches a free phase. Similar features are found for the η and η' results for masses and couplings. Within our scheme we have found that if quark-antiquark bound states persist

beyond the deconfinement transition, they correspond to heavy resonances. Moreover, this unstable mesons interact weakly with its environment.

For the SM case we found similar results for the pion masses in comparison to the SFM approach, namely, the critical baryonic chemical potential increases as a function of the strength of the vector channel G_V . For the kaons we verify that at the confined region, governed by the hadronic model in SM, the mesons in which $S = 1$ (K^- and \bar{K}^0) present a mass decreasing as a function of μ_B , in contrast with the $S = -1$ case, for which both M_{K^+} and M_{K^0} increase with μ_B . The decreasing behavior of the mass is also observed for the η meson at the low baryonic chemical potential region. At the deconfined phase, described by the PNJL0 model at beta equilibrium, a discontinuity is observed, feature also registered for pions and kaons. The comparison with the hadronic output, obtained by using a low order expansion of the chiral interaction as a complement of the DDH δ model, shows that the discontinuity of the masses of the

π , K and η mesons at the transition point is considerable higher than in the PNJL0 model. Furthermore, we have found a qualitative agreement for the masses of the K^0 and K^+ fields. For the pions this similitude extends over baryon densities $\rho/\rho_0 < 2.8$, while for the remaining \bar{K}^0 , K^- , and η mesons, the results are not compatible.

ACKNOWLEDGEMENTS

R. M. A. acknowledges the support given by the CONICET of Argentina under the grant PIP-11220200102081CO. O. L. is member of the project INCT-FNA Proc. No. 464898/2014-5 and acknowledges the support provided by both, Conselho Nacional de Desenvolvimento Científico e Tecnológico (CNPq) under Grant No. 312410/2020-4, and Fundação de Amparo à Pesquisa do Estado de São Paulo (FAPESP) under and Grant No. 2022/03575-3 (BPE).

-
- [1] R. S. Hayano and T. Hatsuda, *Rev. Mod. Phys.* **82**, 2949 (2010).
 - [2] H. Hansen, W. M. Alberico, A. Beraudo, A. Molinari, M. Nardi, and C. Ratti, *Phys. Rev. D* **75**, 065004 (2007).
 - [3] W.-j. Fu and Y.-x. Liu, *Phys. Rev. D* **79**, 074011 (2009).
 - [4] H. Abuki, M. Ciminale, R. Gatto, N. D. Ippolito, G. Nardulli, and M. Ruggieri, *Phys. Rev. D* **78**, 014002 (2008).
 - [5] K. Yamazaki and T. Matsui, *Nuclear Physics A* **922**, 237 (2014).
 - [6] P. Costa, M. C. Ruivo, C. A. de Sousa, H. Hansen, and W. M. Alberico, *Phys. Rev. D* **79**, 116003 (2009).
 - [7] U. S. Gupta and V. K. Tiwari, *Phys. Rev. D* **81**, 054019 (2010).
 - [8] C. Ratti, R. Bellwied, M. Cristoforetti, and M. Barbaro, *Phys. Rev. D* **85**, 014004 (2012).
 - [9] R. Bellwied, S. Borsanyi, Z. Fodor, S. D. Katz, and C. Ratti, *Phys. Rev. Lett.* **111**, 202302 (2013).
 - [10] K. A. Bugaev, V. V. Sagun, A. I. Ivanytskyi, D. R. Oliinychenko, E. M. Ilgenfritz, E. G. Nikonov, A. V. Taranenko, and G. M. Zinovjev, *European Physical Journal A* **52**, 227 (2016).
 - [11] M. Di Toro, M. Colonna, V. Greco, and G.-Y. Shao, *European Physical Journal A* **52**, 224 (2016).
 - [12] N. K. Glendenning, *Phys. Rev. D* **46**, 1274 (1992).
 - [13] E. Annala, T. Gorda, A. Kurkela, J. Nättilä, and A. Vuorinen, *Nature Physics* **16**, 907 (2020).
 - [14] E. Annala, T. Gorda, J. Hirvonen, O. Komoltsev, A. Kurkela, J. Nättilä, and A. Vuorinen, *Nature Communications* **14**, 8451 (2023).
 - [15] A. Barducci, R. Casalbuoni, G. Pettini, and L. Ravagli, *Phys. Rev. D* **71**, 016011 (2005).
 - [16] T. Schäfer, *Phys. Rev. Lett.* **85**, 5531 (2000).
 - [17] H. Basler and M. Buballa, *Phys. Rev. D* **81**, 054033 (2010).
 - [18] J. Steinheimer, S. Schramm, and H. Stöcker, *Journal of Physics G: Nuclear and Particle Physics* **38**, 035001 (2011).
 - [19] S. Benić, I. Mishustin, and C. Sasaki, *Phys. Rev. D* **91**, 125034 (2015).
 - [20] O. A. Mattos, T. Frederico, C. H. Lenzi, M. Dutra, and O. Lourenço, *Phys. Rev. D* **104**, 116001 (2021).
 - [21] O. A. Mattos, O. Lourenço, and T. Frederico, *Journal of Physics: Conference Series* **1291**, 012031 (2019).
 - [22] O. A. Mattos, T. Frederico, and O. Lourenço, *European Physical Journal C* **81**, 24 (2021).
 - [23] J. A. Pons, J. A. Miralles, M. Prakash, and J. M. Lattimer, *The Astrophysical Journal* **553**, 382 (2001).
 - [24] V. Vijayan, N. Rahman, A. Bauswein, G. Martínez-Pinedo, and I. L. Arbina, *Phys. Rev. D* **108**, 023020 (2023).
 - [25] D. Yakovlev and C. Pethick, *Annual Review of Astronomy and Astrophysics* **42**, 169 (2004).
 - [26] E. Friedman and A. Gal, *Physics Reports* **452**, 89 (2007).
 - [27] T. Muto, T. Maruyama, and T. Tatsumi, *Phys. Rev. C* **79**, 035207 (2009).
 - [28] A. Cieplý, E. Friedman, A. Gal, and J. Mareš, *Nuclear Physics A* **925**, 126 (2014).
 - [29] C. Y. Song, X. H. Zhong, L. Li, and P. Z. Ning, *Europhysics Letters* **81**, 42002 (2008).
 - [30] H. Nagahiro, D. Jido, and S. Hirenzaki, *Phys. Rev. C* **80**, 025205 (2009).
 - [31] H. Nagahiro, D. Jido, H. Fujioka, K. Itahashi, and S. Hirenzaki, *Phys. Rev. C* **87**, 045201 (2013).
 - [32] D. Jido, H. Masutani, and S. Hirenzaki, *Progress of Theoretical and Experimental Physics* **2019**, 053D02 (2019).
 - [33] L. Tolos and L. Fabbietti, *Progress in Particle and Nuclear Physics* **112**, 103770 (2020).
 - [34] N. K. Glendenning and J. Schaffner-Bielich, *Phys. Rev. Lett.* **81**, 4564 (1998).
 - [35] A. Mishra, A. Kumar, S. Sanyal, V. Dexheimer, and S. Schramm, *European Physical Journal A* **45**, 169 (2010).
 - [36] T. Maruyama, T. Muto, T. Tatsumi, K. Tsushima, and A. W. Thomas, *Nuclear Physics A* **760**, 319 (2005).

- [37] X. H. Zhong, G. X. Peng, L. Li, and P. Z. Ning, *Phys. Rev. C* **73**, 015205 (2006).
- [38] R. Kumar and A. Kumar, *Phys. Rev. C* **102**, 065207 (2020).
- [39] C. Ratti, M. A. Thaler, and W. Weise, *Phys. Rev. D* **73**, 014019 (2006).
- [40] C. Ratti, S. Rößner, M. A. Thaler, and W. Weise, *European Physical Journal C* **49**, 213 (2007).
- [41] K. Fukushima, *Phys. Rev. D* **77**, 114028 (2008).
- [42] S. Rößner, C. Ratti, and W. Weise, *Phys. Rev. D* **75**, 034007 (2007).
- [43] T. Gaitanos, M. Di Toro, S. Typel, V. Baran, C. Fuchs, V. Greco, and H. Wolter, *Nuclear Physics A* **732**, 24 (2004).
- [44] S. S. Avancini, L. Brito, J. R. Marinelli, D. P. Menezes, M. M. W. de Moraes, C. Providência, and A. M. Santos, *Phys. Rev. C* **79**, 035804 (2009).
- [45] M. Fortin, C. Providência, A. R. Raduta, F. Gulminelli, J. L. Zdunik, P. Haensel, and M. Bejger, *Phys. Rev. C* **94**, 035804 (2016).
- [46] S. P. Klevansky, *Rev. Mod. Phys.* **64**, 649 (1992).
- [47] P. Rehberg, S. P. Klevansky, and J. Hüfner, *Phys. Rev. C* **53**, 410 (1996).
- [48] P. Costa, M. C. Ruivo, C. A. de Sousa, and Y. L. Kalinovsky, *Phys. Rev. C* **70**, 025204 (2004).
- [49] G. Brown, V. Koch, and M. Rho, *Nuclear Physics A* **535**, 701 (1991).
- [50] R. Rapp, R. Machleidt, J. W. Durso, and G. E. Brown, *Phys. Rev. Lett.* **82**, 1827 (1999).
- [51] G. E. Brown and M. Rho, *Phys. Rev. Lett.* **66**, 2720 (1991).
- [52] K. Saito, T. Maruyama, and K. Soutome, *Phys. Rev. C* **40**, 407 (1989).
- [53] D. Kaplan and A. Nelson, *Physics Letters B* **175**, 57 (1986).
- [54] G. Brown, C.-H. Lee, M. Rho, and V. Thorsson, *Nuclear Physics A* **567**, 937 (1994).
- [55] S. Weinberg, *Phys. Rev. Lett.* **18**, 188 (1967).
- [56] P. Papazoglou, S. Schramm, J. Schaffner-Bielich, H. Stöcker, and W. Greiner, *Phys. Rev. C* **57**, 2576 (1998).
- [57] P. Costa and R. C. Pereira, *Symmetry* **11**, 507 (2019), [arXiv:1904.05805 \[hep-ph\]](https://arxiv.org/abs/1904.05805).
- [58] V. Bernard and U. G. Meissner, *Phys. Rev. D* **38**, 1551 (1988).
- [59] C. A. de Sousa and M. C. Ruivo, *Nucl. Phys. A* **625**, 713 (1997).